

## Observations of $CP$ violation in the decays of $B^0$ and $B_s^0$ mesons to two charged pions or kaons

D. MANUZZI

*Dipartimento di Fisica, Università di Bologna - Bologna, Italy*

received 14 February 2022

**Summary.** — The latest measurements of the  $CP$ -violation observables in the charmless two-body decays of  $B^0$  and  $B_s^0$  mesons are reported. The analysis involves the data collected by the LHCb experiment at a centre-of-mass energy of 13 TeV, corresponding to a total integrated luminosity of  $1.9 \text{ fb}^{-1}$ . The combination of these results with the previous determinations by LHCb (additional  $3.1 \text{ fb}^{-1}$ ) provides the most precise measurements of these quantities by a single experiment. In particular, time-dependent  $CP$  violation is observed for the first time in the  $B_s^0$  sector.

### 1. – Introduction

The discovery of the noninvariance of the fundamental interactions for the combined actions of the charge-conjugation ( $C$ ) and parity ( $P$ ) transformations marked an unexpected breakthrough in the development of the Standard Model (SM). So far,  $CP$ -violation phenomena have been measured in several neutral and charged mesons systems [1]. The LHCb experiment [2] provided the first observations of  $CP$  violation in the decay for the  $B^+$ ,  $B_s^0$ , and  $D^0$  mesons [3]. This report presents the latest step of this line: the first observation of time-dependent  $CP$  violation in the  $B_s^0$  sector [4]. The measurement concerns the decays of the  $B_{(s)}^0$  mesons to two charged pions or kaons ( $B_{(s)}^0 \rightarrow h^+ h'^-$ , where  $h, h' \in \{\pi, K\}$ ). Due to the charmless final state, the contributions of tree-level Feynman diagrams to the total amplitudes are suppressed. Thus, loop-level contributions—for instance the ones from “penguin” Feynman diagrams [5]—become relevant. Physics beyond the SM may emerge through virtual contributions inside these loops. The SM encodes the  $CP$ -violation phenomena thanks to the Cabibbo-Kobayashi-Maskawa matrix ( $V_{\text{CKM}}$ ) [6]. A notorious and stringent constraint between the  $V_{\text{CKM}}$  elements is known as *the Unitary Triangle* (UT) [7]. The  $CP$  violation observables of the  $B_{(s)}^0 \rightarrow h^+ h'^-$  decays can be used to determine the angles  $\gamma$  and  $\alpha$  of the UT [8], as well as the  $B_s^0$  mixing phase  $\beta_s$ . Any deviation of these determinations, as compared to the ones obtained with tree-level-dominated transitions, would potentially reveal physics beyond the SM. The time-integrated  $CP$  asymmetries of the  $B^0 \rightarrow K^+ \pi^-$  and  $B_s^0 \rightarrow \pi^+ K^-$  decays can be written as

$$A_{CP}^{B_{(s)}^0} = \frac{|\bar{A}_{\bar{f}}|^2 - |A_f|^2}{|\bar{A}_{\bar{f}}|^2 + |A_f|^2},$$

where  $A_f$  is the amplitude of the flavour-specific decay of a  $B^0$  ( $B_s^0$ ) meson into the final state  $f = K^+\pi^-$  ( $f = \pi^+K^-$ ) and  $\bar{A}_f$  is the amplitude of the  $CP$ -conjugated process. Assuming  $CPT$  invariance and negligible  $CP$  violation in the  $B_{(s)}^0$ - $\bar{B}_{(s)}^0$  mixing, the time-dependent  $CP$  asymmetries of the  $B^0 \rightarrow \pi^+\pi^-$  and  $B_s^0 \rightarrow K^+K^-$  decays are

$$A_{CP}(t) = \frac{\Gamma_{\bar{B}_{(s)}^0 \rightarrow f}(t) - \Gamma_{B_{(s)}^0 \rightarrow f}(t)}{\Gamma_{\bar{B}_{(s)}^0 \rightarrow f}(t) + \Gamma_{B_{(s)}^0 \rightarrow f}(t)} = \frac{-C_f \cos(\Delta m_{d,s}t) + S_f \sin(\Delta m_{d,s}t)}{\cosh\left(\frac{\Delta\Gamma_{d,s}t}{2}\right) + A_f^{\Delta\Gamma} \sinh\left(\frac{\Delta\Gamma_{d,s}t}{2}\right)},$$

where the final state  $f = \pi^+\pi^-$  ( $f = K^+K^-$ ) is a  $CP$  eigenstate, while  $\Delta m_{d,s}$  and  $\Delta\Gamma_{d,s}$  are the mass and width differences of the mass eigenstates in the  $B_{(s)}^0$ - $\bar{B}_{(s)}^0$  two-state systems. The parameters  $C_f$  and  $S_f$  encodes the  $CP$  violation in the decay and in interference between mixing and decay, respectively. The  $A_f^{\Delta\Gamma}$  parameter is related to them by the constraint  $\Sigma_f \equiv \sqrt{(C_f)^2 + (S_f)^2 + (A_f^{\Delta\Gamma})^2} = 1$ , which is not imposed in this analysis, but checked *a posteriori* as an SM consistency test.

## 2. – Data composition

The analysis utilises the data sample of proton-proton collisions at the centre-of-mass energy of 13 TeV collected by LHCb in 2015 and 2016. The total integrated luminosity is about  $1.9\text{fb}^{-1}$ . The  $B_{(s)}^0$  candidates are reconstructed and selected by a dedicated software trigger. The selection algorithm imposes requirements on the quality of the reconstructed tracks, on their kinematic, and on the geometry of the decay candidates. Particle-identification information (PID) is used to separate samples corresponding to the four exclusive final states:  $\pi^+\pi^-$ ,  $K^+K^-$ ,  $K^\pm\pi^\mp$ . The PID performance of LHCb [9] is such that the cross-contamination between the signal channels (*cross-feed background*) is reduced below the 10% of the corresponding signal, keeping adequate efficiency. Besides, a Boosted-Decision-Tree algorithm [10], involving kinematic and geometrical variables, is developed to improve the rejection of the random association of final-state tracks (*combinatorial background*). The partial reconstruction of  $B_{(s)}$  decays to more than two bodies generates the *3-body background*. The good invariant mass resolution of LHCb [9] restricts the large part of this component out of the signal peak.

## 3. – Analysis strategy

The  $CP$ -violation observables  $A_{CP}^{B^0}$ ,  $A_{CP}^{B_s^0}$ ,  $C_{\pi\pi}$ ,  $S_{\pi\pi}$ ,  $C_{KK}$ ,  $S_{KK}$ ,  $A_{KK}^{\Delta\Gamma}$  are extracted from the data with an unbinned maximum-likelihood fit<sup>(1)</sup>. The fit observables are the invariant mass of the two final-state hadrons, the decay time of the  $B_{(s)}^0$  candidates, and the flavour-tagging decision and per-candidate mistag probabilities. The invariant mass is essential to disentangle the signal and background yields. The decay time provides necessary information for the time-dependent  $CP$  asymmetries. The flavour tagging is a set of algorithms exploited to discriminate between  $B_{(s)}^0$  and  $\bar{B}_{(s)}^0$  candidates at the instant of their production [11]. The fit of the four exclusive final-state samples is simultaneous. This feature permits the cross-feed backgrounds to be better handled, although the proximity between their invariant-mass peaks and the signal ones. The

---

<sup>(1)</sup> The parameter  $A_{\pi\pi}^{\Delta\Gamma}$  is not measured because of the almost null value of  $\Delta\Gamma_d$  [1].

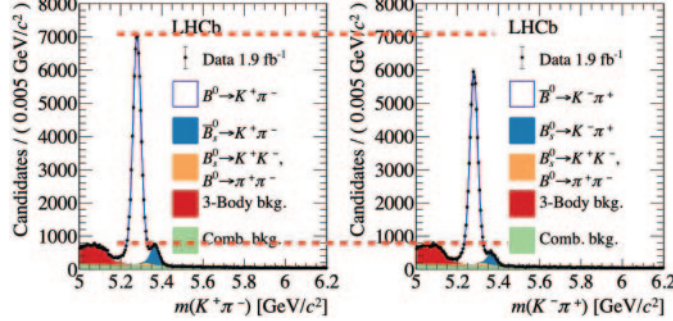


Fig. 1. – Invariant mass for the  $K^+\pi^-$  (left) and  $\pi^+K^-$  (right) final states. The projection of the best fit is superimposed. The red dashed lines remark the different yields of the signal modes [4].

fit model considers several experimental effects, which are now briefly introduced. Since LHC is a proton-proton collider, the production cross sections of  $B_{(s)}^0$  and  $\bar{B}_{(s)}^0$  mesons are not guaranteed to be equal. This *production asymmetry* is handled thanks to the decay-time information about the  $B^0 \rightarrow K^+\pi^-$  decays. The time-integrated  $CP$  asymmetries are biased by the so called *final-state asymmetries*, which are due to the slightly different detection and identification efficiency of opposite-charged particles. The corresponding correction is determined using  $D^0 \rightarrow K^-\pi^+$ ,  $D^+ \rightarrow K^-\pi^+\pi^-$ , and  $D^+ \rightarrow \bar{K}^0\pi^+$  decays. Wrong *flavour-tagging decisions* dilute the time-dependent  $CP$  asymmetries. The flavour-tagging algorithms provide a raw expectation of the mistag probability for each candidate. This quantity is calibrated directly in the final fit exploiting the flavour-specific  $B^0 \rightarrow K^+\pi^-$  and –to a minor extent–  $B_s^0 \rightarrow \pi^+K^-$  decay modes. Another source of dilution is due to the *decay-time resolution*. Studies on  $J/\psi \rightarrow \mu^+\mu^-$  and  $\Upsilon(4S) \rightarrow \mu^+\mu^-$  decays and fully simulated  $B_s^0 \rightarrow K^+K^-$  decays allow the decay-time resolution for the  $B_{(s)}^0 \rightarrow h^+h^-$  decays to be determined and considered in the fit. The reconstruction efficiency of the signal candidates depends on their decay time. Hence, the fit model includes effective efficiency functions. Their extraction starts from a background-subtracted  $B^0 \rightarrow K^+\pi^-$  sample: when the flavour-tagging decision is neglected, its decay-time shape is the product of an exponential with the decay-time efficiency.

#### 4. – Results

Figure 1 shows the invariant-mass distributions for the  $K^+\pi^-$  and  $\pi^+K^-$  final-states samples, evidencing the difference between the yields of the  $CP$ -conjugated signal modes. Figure 2 illustrates the time-dependent  $CP$  asymmetries as obtained from the data in the invariant mass region dominated by the signal component. In both the figures, the results of the best fits are superimposed. The results of this analysis are:

$$\begin{aligned}
 A_{CP}^{B^0} &= (-8.24 \pm 0.33 \pm 0.33)\%, & C_{\pi\pi} &= (-31.1 \pm 4.5 \pm 1.5)\%, & C_{KK} &= (+16.4 \pm 3.4 \pm 1.4)\%, \\
 A_{CP}^{B_s^0} &= (+23.6 \pm 1.3 \pm 1.1)\%, & S_{\pi\pi} &= (-70.6 \pm 4.2 \pm 1.3)\%, & S_{KK} &= (+12.3 \pm 3.4 \pm 1.5)\%, \\
 A_{KK}^{\Delta\Gamma} &= (-83 \pm 5 \pm 9)\%.
 \end{aligned}$$

where the reported uncertainties are statistic and systematic, respectively. The systematic uncertainties are always smaller than the corresponding statistical uncertainties, except for  $A_{KK}^{\Delta\Gamma}$ , which is mainly affected by external inputs ( $\Delta m_s$ ,  $\Delta\Gamma_s$ ) and limited size of the sample available to estimate the decay-time efficiencies. These results are compat-

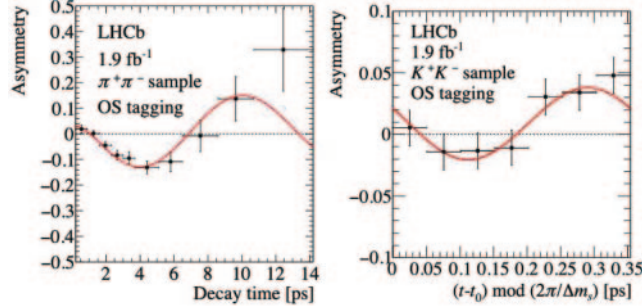


Fig. 2. – Time-dependent  $CP$  asymmetries for  $B^0 \rightarrow \pi^+\pi^-$  (left) and  $B^0 \rightarrow K^+K^-$  decays (right). The data point are obtained from the invariant mass regions  $m(\pi^+\pi^-) \in [5.20, 5.35] \text{ GeV}/c^2$  and  $m(K^+K^-) \in [5.30, 5.44] \text{ GeV}/c^2$ , respectively. The red lines show the results of the best fit [4].

ible with the previous measurements by LHCb (a  $\chi^2$  test statistic provides a  $p$ -value of 0.68) and other experiments [12,13]. The combination of the LHCb determinations is

$$\begin{aligned}
 A_{CP}^{B^0} &= (-8.31 \pm 0.34)\%, & C_{\pi\pi} &= (-32.0 \pm 3.8)\%, & C_{KK} &= (+17.2 \pm 3.1)\%, \\
 A_{CP}^{B_s^0} &= (+22.5 \pm 1.2)\%, & S_{\pi\pi} &= (-67.2 \pm 3.4)\%, & S_{KK} &= (+13.9 \pm 3.2)\%, \\
 A_{KK}^{\Delta\Gamma} &= (-89.7 \pm 8.7)\%.
 \end{aligned}$$

To date, these are the most precise measurements of these quantities from a single experiment. The SM test cited above is satisfied within one standard deviation:  $\Sigma_{KK} = 0.93 \pm 0.08$ . The significance for  $(C_{KK}, S_{KK}, A_{KK}^{\Delta\Gamma}) \neq (0, 0, -1)$  is 6.5 standard deviations. This is the first observation of time-dependent  $CP$  violation in the  $B_s^0$  sector. The just presented results involve a total integrated luminosity of  $5 \text{ fb}^{-1}$ . The same analysis strategy presented in this report is currently employed for updating these measurements with the data collected by LHCb in 2017 and 2018 (further  $4 \text{ fb}^{-1}$ ).

## REFERENCES

- [1] PARTICLE DATA GROUP, *Prog. Theor. Exp. Phys.*, **2020** (2020) 083C01.
- [2] LHCb COLLABORATION, *JINST*, **3** (2008) S08005.
- [3] LHCb COLLABORATION, *Phys. Lett. B*, **713** (2012) 351; *Phys. Rev. Lett.*, **110** (2013) 221601; **122** (2019) 211803.
- [4] LHCb COLLABORATION, *JHEP*, **03** (2021) 075.
- [5] GRONAU M. *et al.*, *Phys. Rev. D*, **50** (1994) 4529; **52** (1995) 6356.
- [6] CABIBBO N., *Phys. Rev. Lett.*, **10** (1963) 531; KOBAYASHI M. and MASKAWA T., *Prog. Theor. Phys.*, **49** (1973) 652.
- [7] UTFIT COLLABORATION, *JHEP*, **10** (2006) 081.
- [8] LHCb COLLABORATION, *Phys. Lett. B*, **739** (2015) 1; FLEISCHER R., *Eur. Phys. J. C*, **52** (2007) 267; CIUCHINI M. *et al.*, *JHEP*, **10** (2012) 029.
- [9] LHCb COLLABORATION, *Int. J. Mod. Phys. A*, **30** (2015) 1530022.
- [10] FREUND Y. and SCHAPIRE R. E., *J. Comput. Syst. Sci.*, **55** (1997) 119.
- [11] LHCb COLLABORATION, *Eur. Phys. J. C*, **72** (2012) 2022; **77** (2017) 238; *JINST*, **10** (2015) P10005; **11** (2016) P05010.
- [12] LHCb COLLABORATION, *Phys. Rev. D*, **98** (2018) 032004.
- [13] BABAR COLLABORATION, *Phys. Rev. D*, **87** (2013) 052009; BELLE COLLABORATION, *Phys. Rev. D*, **88** (2013) 092003; **87** (2013) 031103. CDF COLLABORATION *et al.*, *Phys. Rev. Lett.*, **113** (2014) 242001.